Supplemental Material

Methods for Supplemental Material

Body composition analyses

Mice fed regular chow diets were randomly picked for body mass measurements and body composition analyses. Fat and lean body masses were measured using an EchoMRI-100H Whole Body Composition Analyzer (Echo Medical System) and then obtained values were normalized to body mass. Scans were performed by placing mice in a plastic cylinder to limit movement and took less than 2 min per mouse. Measured fat and lean masses of individual mice were normalized to total body mass.

Quantitative real-time qPCR

Total RNA was extracted from dissected livers from mice 4-6 months of age using the RNeasy Isolation Kit (Qiagen). Quality and concentrations of RNA were measured using a Nanodrop spectrophotometer. The cDNA was synthesized using Superscript First Strand Synthesis System instructions (Thermo Fisher Scientific). For each replicate in each experiment, RNAs from livers of different animals were used (n = 4 per group). The sequences of qPCR primers were either designed using Primer3 software or used with validated primers from the PrimerBank (https://pga.mgh.harvard.edu/primerbank) (1). The primer sequences used for the study are listed in the Supplemental Table 3. PCR was performed on a MX3005p qPCR System (Stratagene) using Brilliant III Ultra Fast SYBR Green qPCR Master Mix (Agilent Technologies, 600883). Relative levels of mRNA expression were calculated using the $\Delta\Delta$CT method (2). Individual expression values were normalized by comparison to GADPH mRNA.

Immunoblotting

Lysates of cultured hepatocytes and livers dissected from mice were homogenized in RIPA Buffer (Cell Signaling) supplemented with 0.1% SDS, 0.2% sodium deoxycholic acid, Protease

Inhibitor Cocktail (Roche) and 1 mM PMSF (Sigma-Aldrich). Proteins in samples were denatured by boiling in Laemmli sample buffer (3) containing β-mercaptoethanol for 5 min, separated by 10% or 4% SDS-PAGE and transferred to nitrocellulose membranes. For immunoblotting, membranes were washed with blocking buffer (PBS containing 5% BSA and 0.2% polysorbate-20) for 30 min and then probed with primary antibodies in blocking buffer overnight at 4^{o}C. Primary antibodies were against LAP1 (4), torsinA (Abcam, ab34540), GRP78 (Cell Signaling, 2177), eIF2 (Cell Signaling, 9722), phospho-eIF2 (Cell Signaling, 9721), CHOP (Santa Cruz Biotechnology, sc-7351), insulin receptor (Cell Signaling, 3025), phospho-insulin receptor (Cell Signaling, 3918), AKT2 (BD transduction, 2694), phosphor-AKT2 (SAB Signalway, 11124) and γ-tubulin (Sigma-Aldrich, T5326). Blots were washed with PBS containing 0.1% polysorbate-20 and then incubated in blocking buffer containing horseradish peroxidase-conjugated secondary antibodies (GE Healthcare) for 1 hour at room temperature. Recognized proteins were visualized by Enhanced Chemiluminescence (Thermo Fisher Scientific) and exposure to X-ray films. To quantify signals, immunoblots were scanned and the densities of the bands quantified using ImageJ software (5).

Analysis of lipids using high performance liquid chromatography-mass spectrometry

Excised livers from mice at 2 months of age were weighed and snap-frozen prior to lipidomic analysis. Lipid extracts were prepared using a modified Bligh and Dyer method (6) and analyzed using a 6490 Triple Quadrupole LC/MS system (Agilent Technologies). Glycerophospholipids were separated with normal-phase HPLC as described before with a few modifications (7). An Agilent Zorbax Rx-Sil column (inner diameter 2.1 x 100 mm) was used under the following conditions: mobile phase A (chloroform:methanol:1 M ammonium hydroxide, 89.9:10:0.1, v/v) and mobile phase B (chloroform:methanol:water:ammonium hydroxide, 55:39.9:5:0.1, v/v); 95% A for 2 min, linear gradient to 30% A over 18 min and held for 3 min, and linear gradient to 95%

A over 2 min and held for 6 min. Quantification of lipid species was accomplished using multiple reaction monitoring transitions and instrument settings that were developed in earlier studies (7) in conjunction with referencing of appropriate internal standards (Avanti Polar Lipids).

References

1. Wang X, Spandidos A, Wang H, Seed, B. Primerbank: A pcr primer database for quantitative gene expression analysis, 2012 update. *Nucleic Acids Res*. 2012;40(Database issue):D1144-D1149.
2. Ponchel F et al. Real-time pcr based on sybr-green i fluorescence: An alternative to the taqman assay for a relative quantification of gene rearrangements, gene amplifications and micro gene deletions. *BMC Biotechnol*. 2003;3:18.
3. Laemmli UK. Cleavage of structural proteins during the assembly of the head of bacteriophage T4. *Nature.* 1970;227(5259):680-685.
4. Goodchild RE, Dauer WT. The AAA+ protein torsinA interacts with a conserved domain present in LAP1 and a novel ER protein. *J Cell Biol*. 2005;168(6):855-862.
5. Schneider CA, Rasband WS, Eliceiri KW. NIH Image to ImageJ: 25 years of image analysis. *Nat Methods*. 2012;9(7):671-675.
6. Bligh EG, Dyer WJ. A rapid method of total lipid extraction and purification. *Can J Biochem Physiol.* 1959; 37(8): 911-917.
7. Chan RB, Oliveira TG, Cortes EP, Honig LS, Duff KE, Small SA, Wenk MR, Shui G, Di Paolo G. Comparative lipidomic analysis of mouse and human brain with Alzheimer disease. *J Biol Chem*. 2012; 287(4): 2678-2688.

Figures and figure legends for Supplemental material

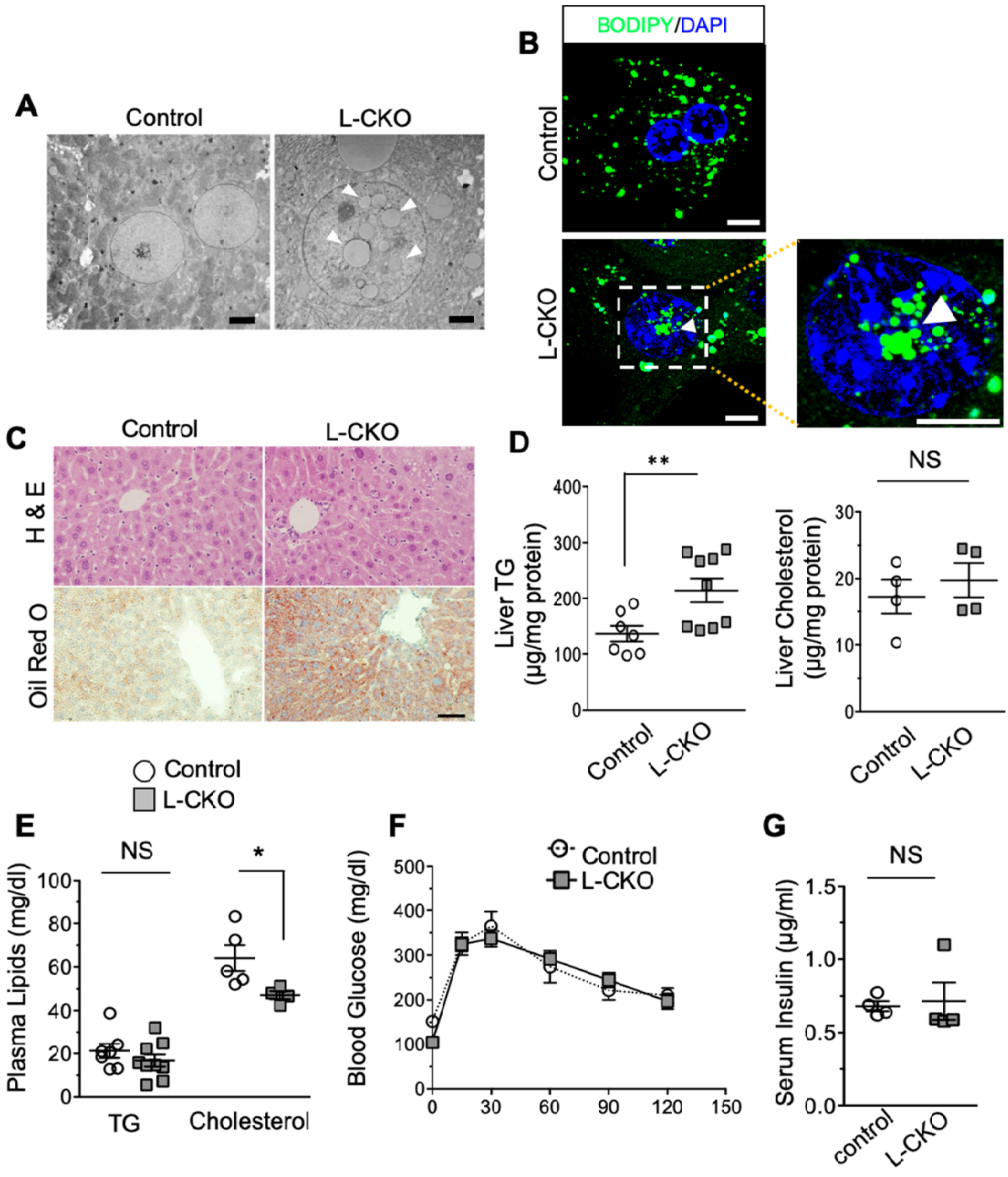

Supplemental Figure 1. Hepatic steatosis without insulin resistance in female L-CKO mice fed a chow diet. (A) Electron micrographs of liver sections from female control (*Tor1aip1*$^{flox/flox}$) and L-CKO (*AlbCre; Tor1aip1*$^{flox/flox}$) mice. White arrowheads indicate

intranuclear lipid droplets. Scale bar: 2 μm. (B) Confocal micrographs of isolated hepatocytes. Lipids were stained with BODIPY (green) and nuclei with DAPI (blue). The right panel is a zoomed image of the dotted square region in the middle panel. White arrowheads indicate intranuclear lipid droplets. Scale bars: 10 μm. (C) Representative light micrographs of liver sections from chow-fed mice stained with H&E (upper panels) and Oil Red O (lower panels). Scale bar: 50 μm. (D) Liver TG and cholesterol contents; mice were fasted for 5 hours before collecting livers, n = 4-9 mice per group. $^{**}P < 0.01$, NS: not significant by Student's t test. (E) Plasma TG and cholesterol concentrations, n = 4-9 mice per group. $^{*}P < 0.05$ by Student's t test. (F) Blood glucose concentration versus time after injection of a glucose bolus in overnight-fasted mice, n = 6 mice per group. Not significantly different at any time point by ANOVA. (G) Serum insulin concentrations. Mice were fasted for 5 hours before collecting plasma, n = 4 mice per group. NS: not significant by Student's t test. In panels D, E and G, values for individual mice are shown with longer horizontal bars representing means and vertical bar representing SEM. Control and L-CKO mice at 4-6 months of age were used.

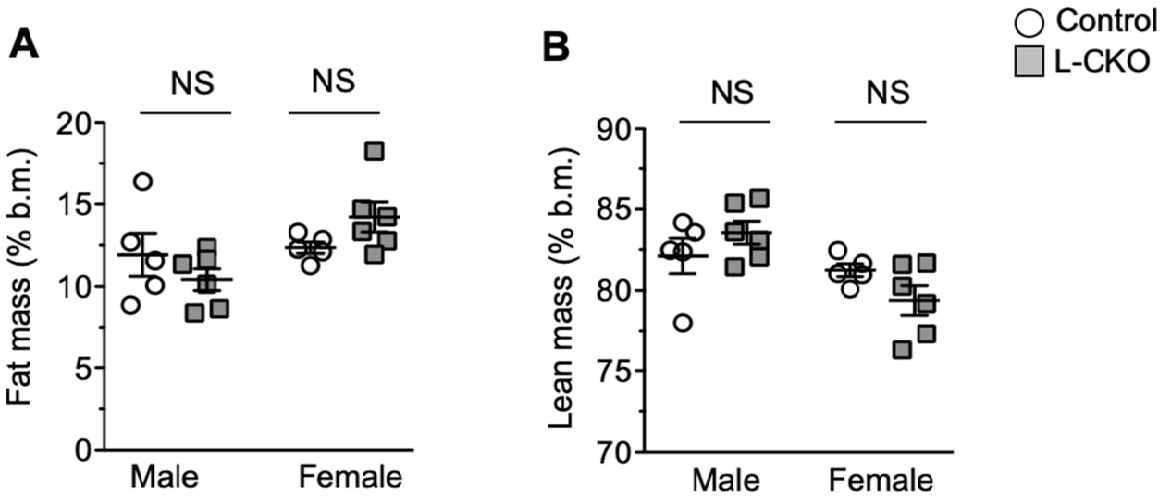

Supplemental Figure 2. Body composition analysis in male and female L-CKO mice fed a chow diet. (A) Total fat mass as percent of body mass (b.m.) of male and female L-CKO and age-matched control mice, n = 5-6 mice per group. N.S not significant by Student's t-test. (B) Total lean mass as percent of body mass (b.m.) of male and female L-CKO and age-matched control mice, n = 5-6 mice per group. N.S not significant by Student's t-test. Values for individual mice are shown with longer horizontal bars representing means and vertical bar representing SEM. Mice at 4 months of age were used.

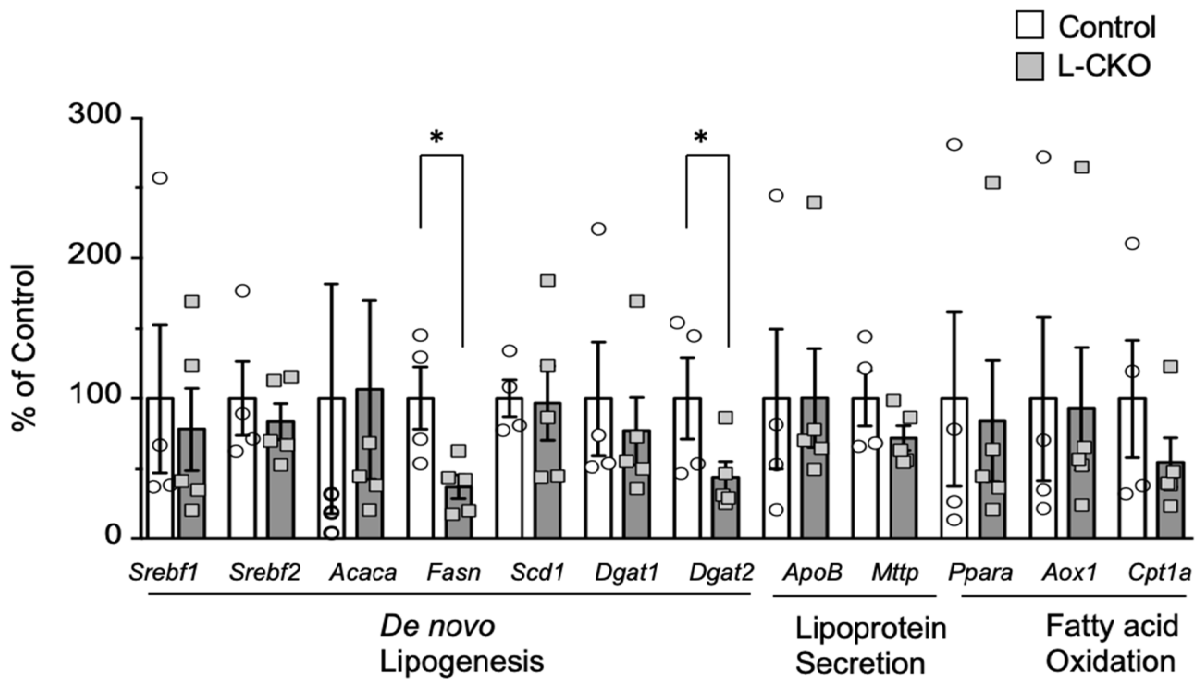

Supplemental Figure 3. Lipid metabolism-related gene expression in L-CKO mice. Expression of select genes involved in liver lipid metabolism in extracts of livers from control and L-CKO mice, n = 4-5 mice per genotype. *P < 0.05 by Student's t test. Values for individual mice are shown with each bar showing the mean ± SEM. Mice at 4-6 months of age were used.

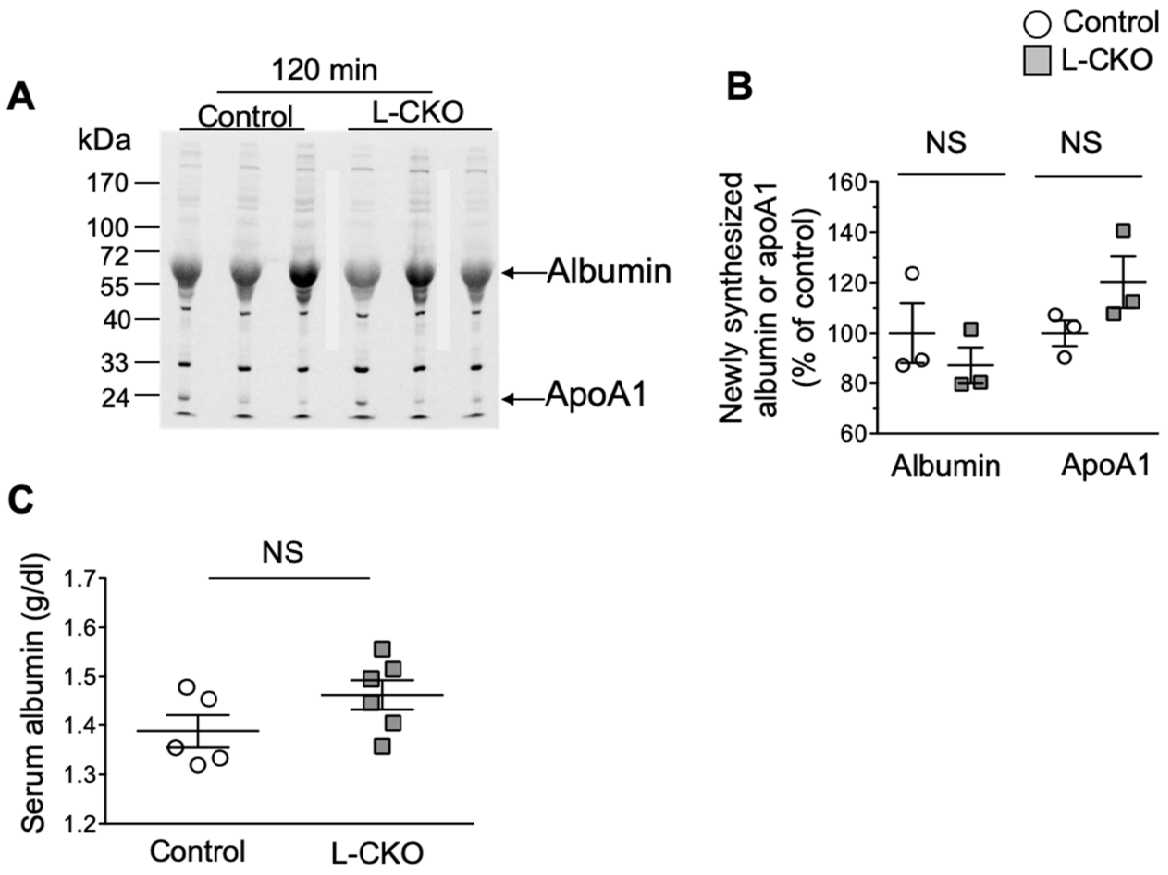

Supplemental Figure 4. Hepatic albumin and apolipoprotein A1 secretion and serum albumin concentrations in L-CKO mice. (A) Autoradiogram of SDS-polyacrylamide gel showing ^{35}S- labeled plasma proteins collected at 120 min after intravenous injection of mice with ^{35}S-methionine. Migrations of molecular mass standards in kDa are indicated at the left. Migrations of ^{35}S-methionine labeled albumin and apolipoprotein A1 (apoA1) are indicated at the right. Each lane shows plasma proteins from an individual mouse. (B) Bands corresponding to albumin and apoA1 shown in panel A were quantified by densitometry, n = 3 per group. NS: not significant by Student's t test, (C) Serum albumin concentrations in control and L-CKO mice, n = 5-6 per genotype, NS: not significant by Student's t-test. In panels B and C, values for individual mice are shown with longer horizontal bars representing means and vertical bar representing SEM. Mice at 4 months of age were used.

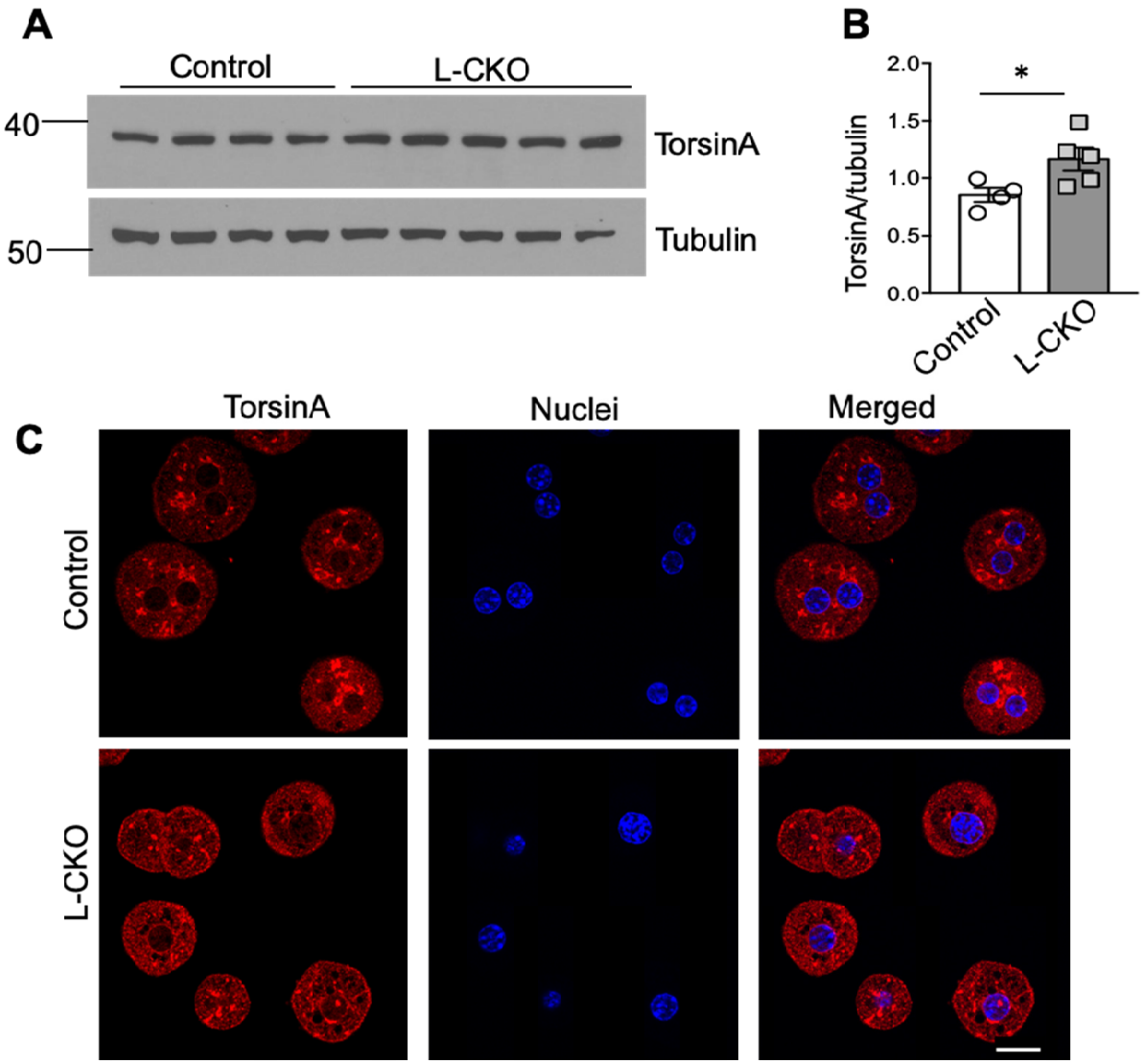

Supplemental Figure 5. TorsinA expression and localization in livers of L-CKO mice. (A) Immunoblots of liver lysates from control and L-CKO mice using anti-torsinA and anti-γ-tubulin Abs. (B) Band densities for indicated proteins were normalized to the band density of γ-tubulin as a loading control. Results are from n = 4 control and n = 5 L-CKO mice. **P* < 0.05 by Student's t test. (C) Confocal immunofluorescence micrographs of isolated hepatocytes from L-CKO and control mice label with anti-torsinA Abs; nuclei are stained with DAPI. TorsinA staining showed an ER-like distribution in hepatocytes from both control and L-CKO mice. Bar :10 μm.

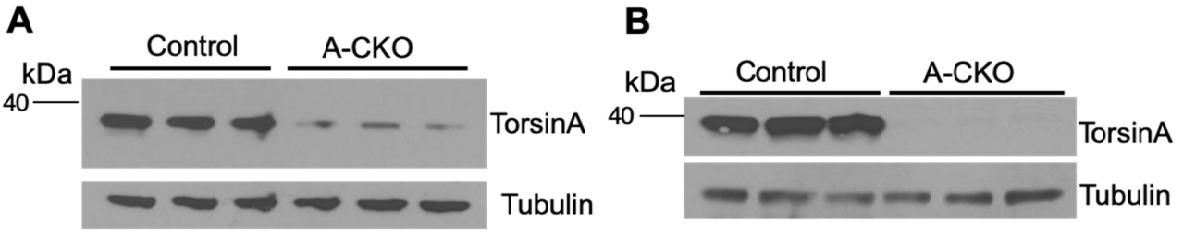

Supplemental Figure 6. Depletion of torsinA in livers and isolated hepatocytes of A-CKO mice. (A) Immunoblot of liver lysates from control (*Tor1a*$^{flox/+}$) and A-CKO (*AlbCre; Tor1a*$^{flox/-}$) mice probed with Abs against torsinA and γ-tubulin. Each lane contains lysates from an individual mouse. (B) Immunoblot of hepatocyte cell lysates from control and A-CKO mice probed with Abs against torsinA and γ-tubulin. Each lane contains 3 different wells of hepatocyte lysates from one mouse per each genotype. Immunoblot probe with Ab against gamma tubulin is shown as loading control. Migrations of molecular mass standards are indicated at the left. Mice at 4months of age were used.

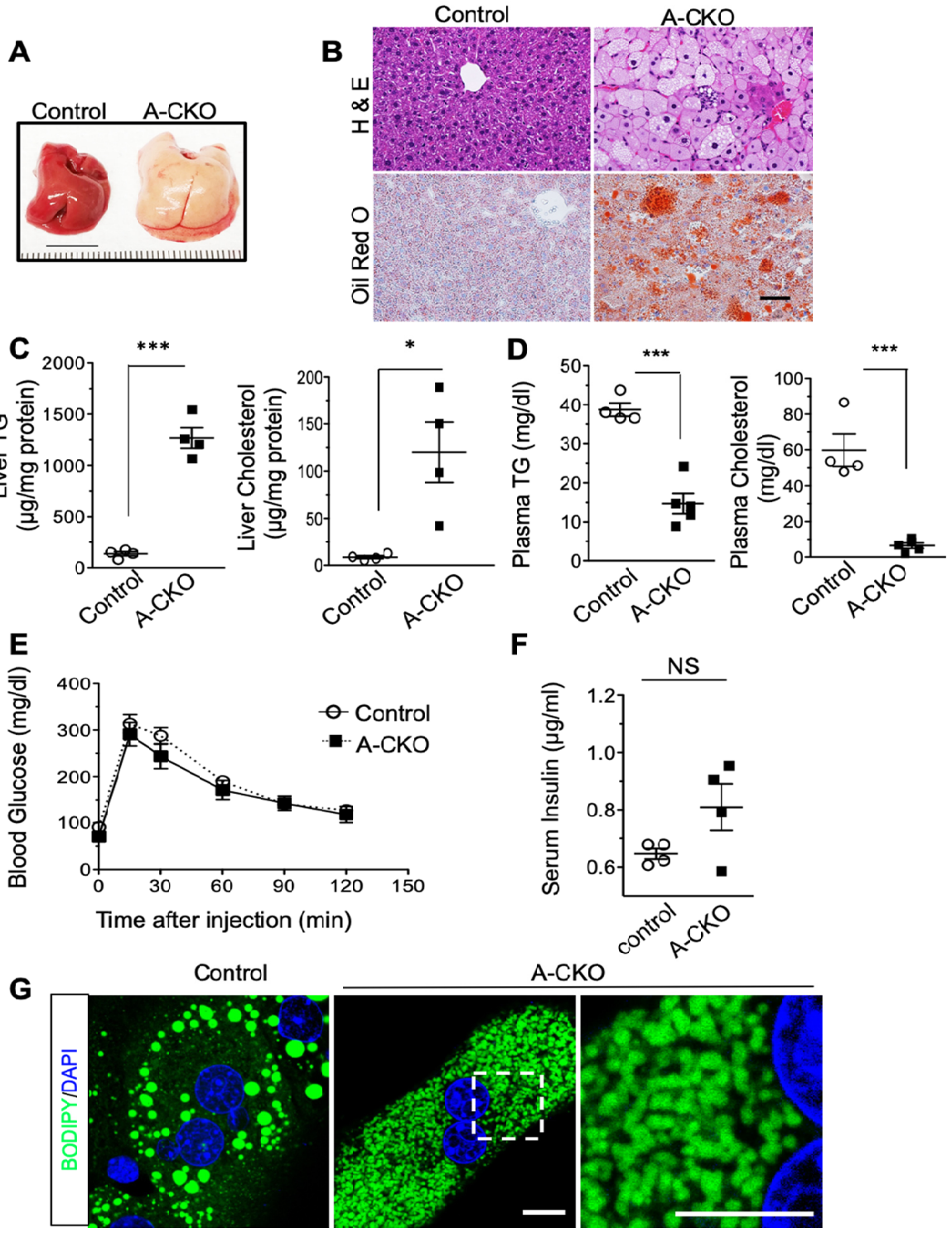

Supplemental Figure 7. Hepatic steatosis without insulin resistance in female A-CKO mice fed a chow diet. (A) Photographs of livers of female control and A-CKO mice fed chow

diet. Bar: 1 cm (B) Representative light micrographs of liver sections from chow-fed mice stained with H&E (upper panel) and Oil Red O (bottom panel). Scale bar: 50 μm. (C) Liver TG and cholesterol contents; mice were fasted for 5 hours before collecting livers, n = 4-5 per group. *P < 0.001, ***P < 0.001 by Student's t test. (D) Plasma TG and cholesterol concentrations, n = 4-5 per group. ***P < 0.001 by Student's t test. (E) Blood glucose concentration versus time after injection of a glucose bolus in overnight-fasted mice. Values are means ± SEM, n = 5 per group. Not significantly different at any time point by ANOVA. (F) Serum insulin concentrations. Mice were fasted for 5 hours before collecting plasma, n = 4 mice per group. NS: not significant by Student's t test. (G) Confocal micrographs of isolated hepatocytes. Lipids were stained with BODIPY (green) and nuclei with DAPI (blue). The right panel is a zoomed image of the dotted rectangular region. Scale bars: 10 μm. In panels C, D and F, values for individual mice are shown with longer horizontal bars representing means and vertical bar representing SEM in panels. Mice at 6 months of age were used.

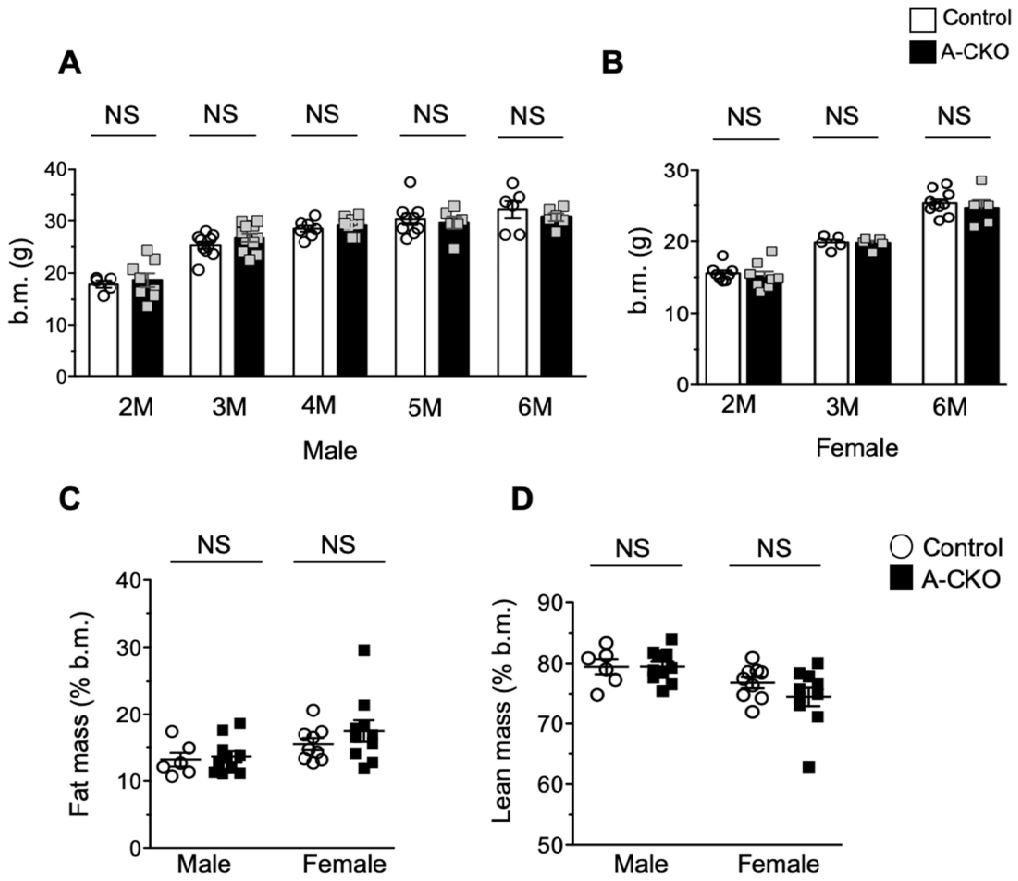

Supplemental Figure 8. Body mass and composition analysis in male and female A-CKO mice fed a chow diet. (A) Body mass (b.m.) of male control and A-CKO mice, n = 8-10 mice per group. N.S. not significant by Student's t-test. (B) Body mass of female control and A-CKO mice, n = 5-8 mice per group. N.S. not significant by Student's t-test. (C) Total fat mass as percent of body mass (b.m.) measured of male and female A-CKO and control mice, n = 6-10 mice per group. N.S. not significant by Student's t-test. (D) Total lean mass as percent of body mass of male and female A-CKO and age-matched control mice, n = 6-10 mice per group. N.S. not significant by Student's t-test. In panels A and B, values for individual mice are shown with each bar showing the mean ± SEM. In panels C and D, values for individual mice are shown with longer horizontal bars representing means and vertical bar representing SEM. Mice at 4-6 months of age were used. Mice at 2-6 months of age were used.

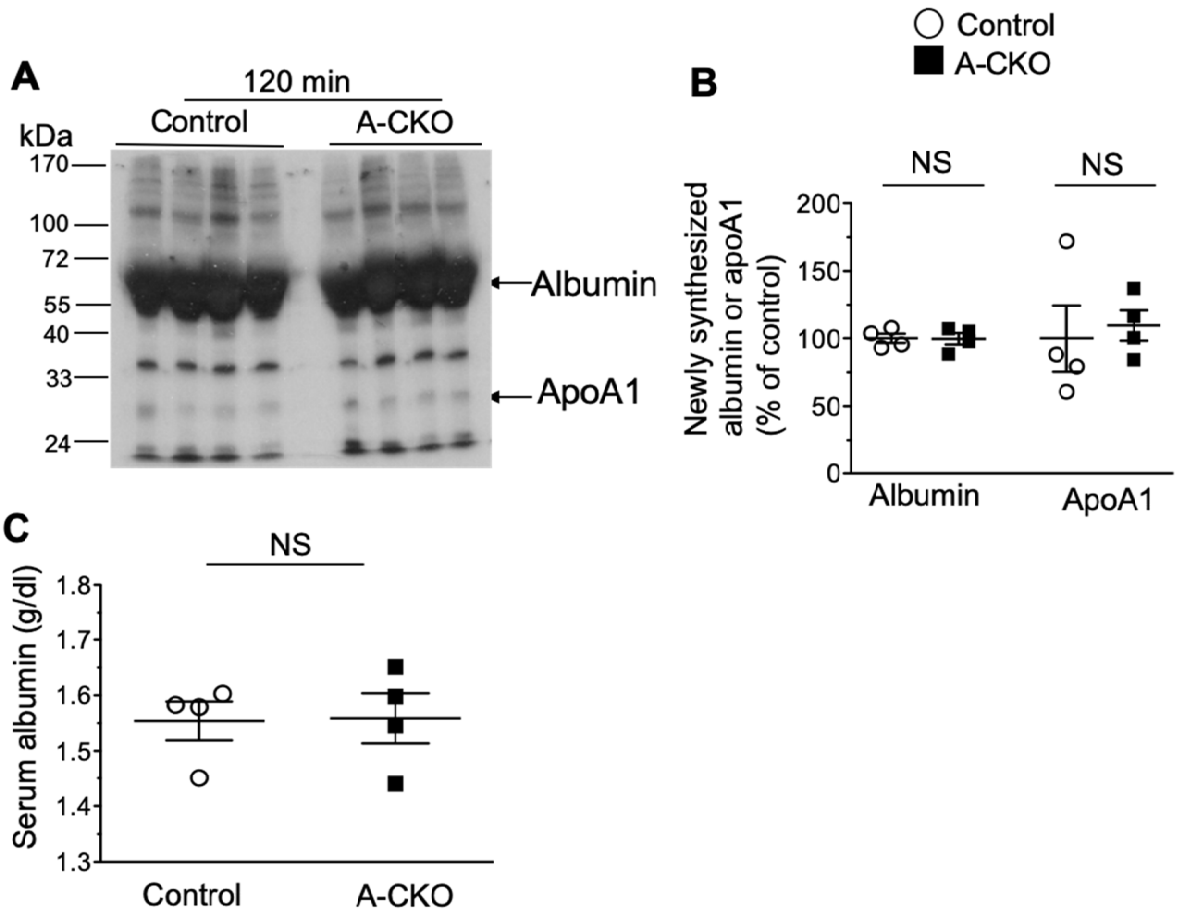

Supplemental Figure 9. Hepatic albumin and apolipoprotein A1 secretion and serum albumin concentrations in A-CKO mice. (A) Autoradiogram of SDS-polyacrylamide gel showing ^{35}S-labeled plasma proteins collected at 120 min after intravenous injection of mice with ^{35}S-methionine. Migrations of molecular mass standards are indicated at the left. Migrations of ^{35}S-labeled albumin and apolipoprotein A1 (apoA1) are indicated at the right. Each lane shows plasma proteins from an individual mouse. (B) Bands corresponding to albumin and apoA1 shown in panel A were quantified by densitometry, n = 4 per group. NS: not significant by Student's t test. (C) Serum albumin concentrations in control and A-CKO mice, n = 4 per group, NS: not significant by Student's t-test. In panels B and C, values for individual mouse are shown with longer horizontal bars representing means and vertical bar representing SEM. Mice at 4 months of age were used.

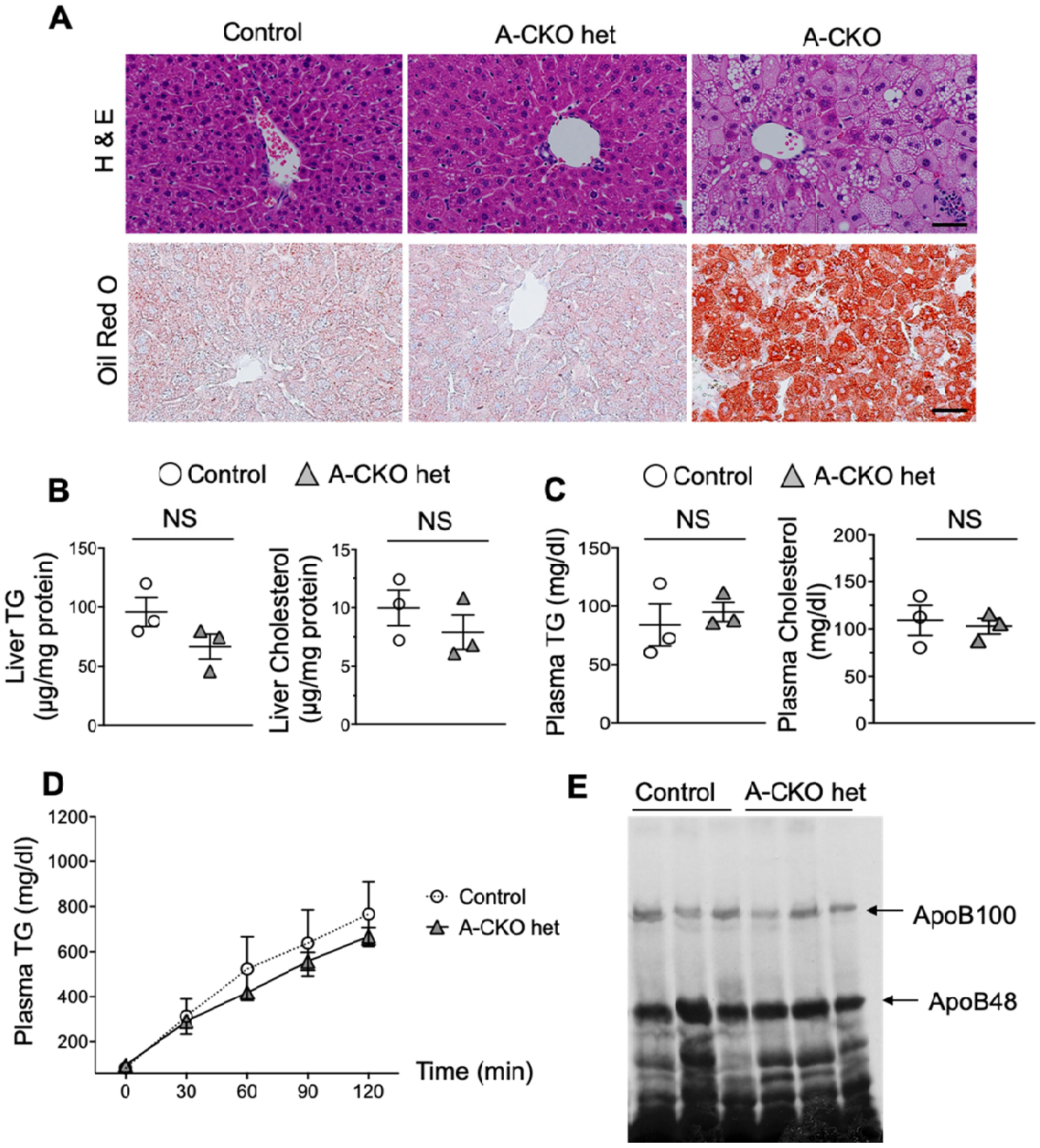

Supplemental Figure 10. Mice heterozygous for hepatocyte *Tor1a* deletion do not have hepatic steatosis or decreased VLDL secretion. (A) Representative light micrographs of liver sections from chow-fed control (*Tor1a*$^{flox/+}$), A-CKO het (*AlbCre; Tor1a*$^{flox/+}$) and A-CKO (*AlbCre; Tor1a*$^{flox/-}$) mice stained with H&E (upper panels) and Oil Red O (bottom panels). Scale bar: 50 µm. (B) Liver TG and cholesterol content of control and A-CKO het mice; mice were fasted for

5 hours before collecting livers, n = 3 per group. NS: not significant by Student's t test. (C) Plasma TG and cholesterol concentrations, n = 3 per group. NS: not significant by Student's t test. (D) Control and A-CKO het mice were injected with tyloxapol to block peripheral TG uptake and plasma concentrations measured at times indicated. Values are means ± SEM, n = 3 mice per group. (E) Autoradiogram of SDS-polyacrylamide gel showing ^{35}S-labeled plasma proteins collected 120 min after injection with ^{35}S-methionine. Each lane shows proteins from an individual mouse. Migrations of ^{35}S-methionine labeled apoB100 and apoB48 are indicated.

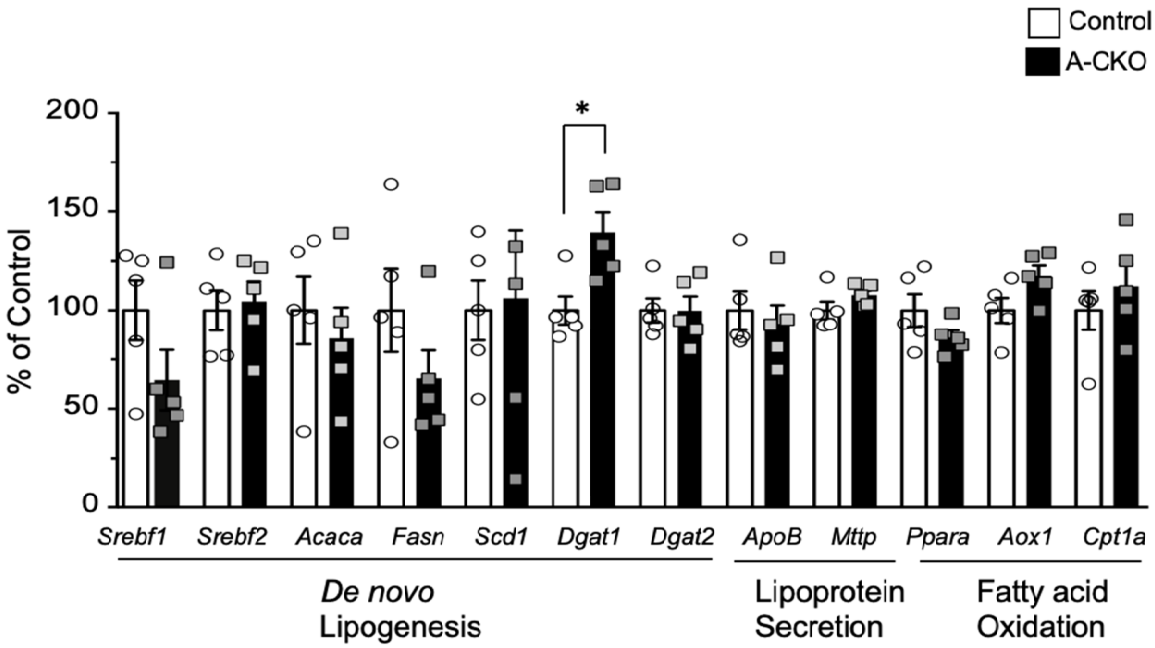

Supplemental Figure 11. Lipid metabolism-related gene expression in A-CKO mice. Expression of select genes involved in liver lipid metabolism in extracts of livers from control and A-CKO mice, n = 5 mice per genotype. *P < 0.05 by Student's t test. Values for individual mice are shown with each bar showing the mean ± SEM. Mice at 4-6 months of age were used.

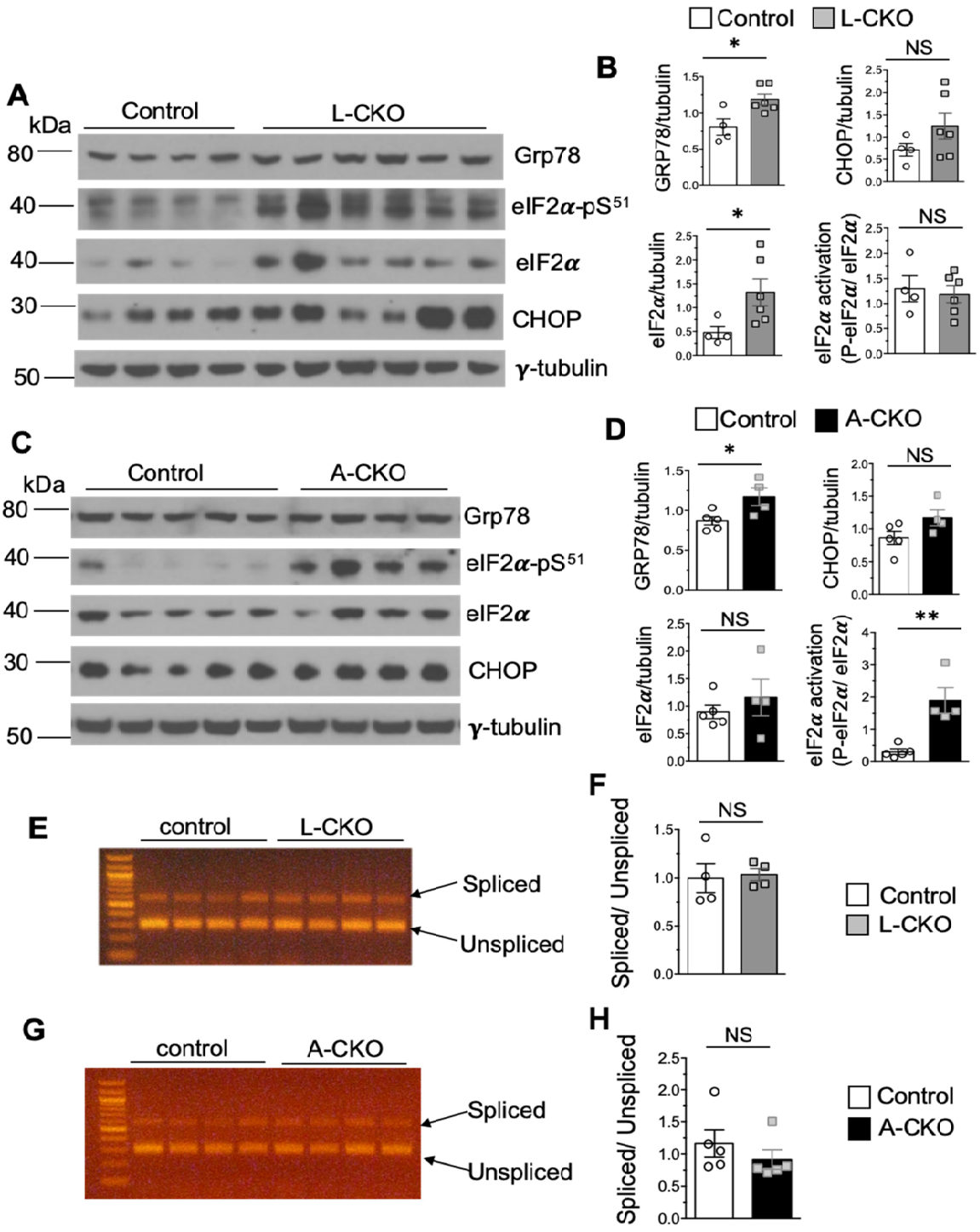

Supplemental Figure 12. ER stress response in livers of L-CKO and A-CKO mice. (A) Immunoblots of liver lysates from control and L-CKO mice using Abs to detect indicated ER stress-related proteins. (B) Band densities of indicated proteins were normalized to the band

density of γ-tubulin. Activation of eIF2α was calculated from the ratio of p-eIF2α/total eIF2α signals. Results are from n = 4 control and n = 6 L-CKO mice. *P < 0.05, NS: not significant by Student's t test. (C) Immunoblots of liver lysates from control and A-CKO mice using Abs to detect indicated ER stress-related proteins. (D) Band densities for indicated proteins were normalized to the band density of γ-tubulin as a loading control. Activation of eIF2α was calculated from the ratio of p-eIF2α/ total eIF2α signals. Results are from n = 5 control and n = 4 L-CKO mice. *P < 0.05, **P < 0.01, NS: not significant by Student's t test. (E) Ethidium bromide-stained agarose gels of XBP1 RT-PCR products followed by Pst1 endonuclease digestion of cDNA synthesized from total RNAs isolated from control and L-CKO mouse livers. Unspliced (300 bp) and spliced (574 bp) cDNAs are indicated by arrows, n = 4 per group. (F) Band density ratios of spliced and unspliced XBP1 measured from the gel in panel A. NS: not significant by Student's t test. In panels B, D values for individual mice are shown with longer horizontal bars representing means and vertical bar representing. Mice at 6 months of age were used. (G) Ethidium bromide-stained agarose gel of XBP1 RT-PCR products followed by Pst1 endonuclease digestion of cDNAs synthesized from total RNAs isolated from control and A-CKO mouse livers. Unspliced (300 bp) and spliced (574 bp) cDNAs are indicated by arrows, n = 4 per group. (H) Band density ratios of spliced and unspliced XBP1 measured from the gel in panel A. NS: not significant by Student's t test. In panels B and D values for individual mice are shown with each bar showing the mean ± SEM . Mice at 6 months of age were used.

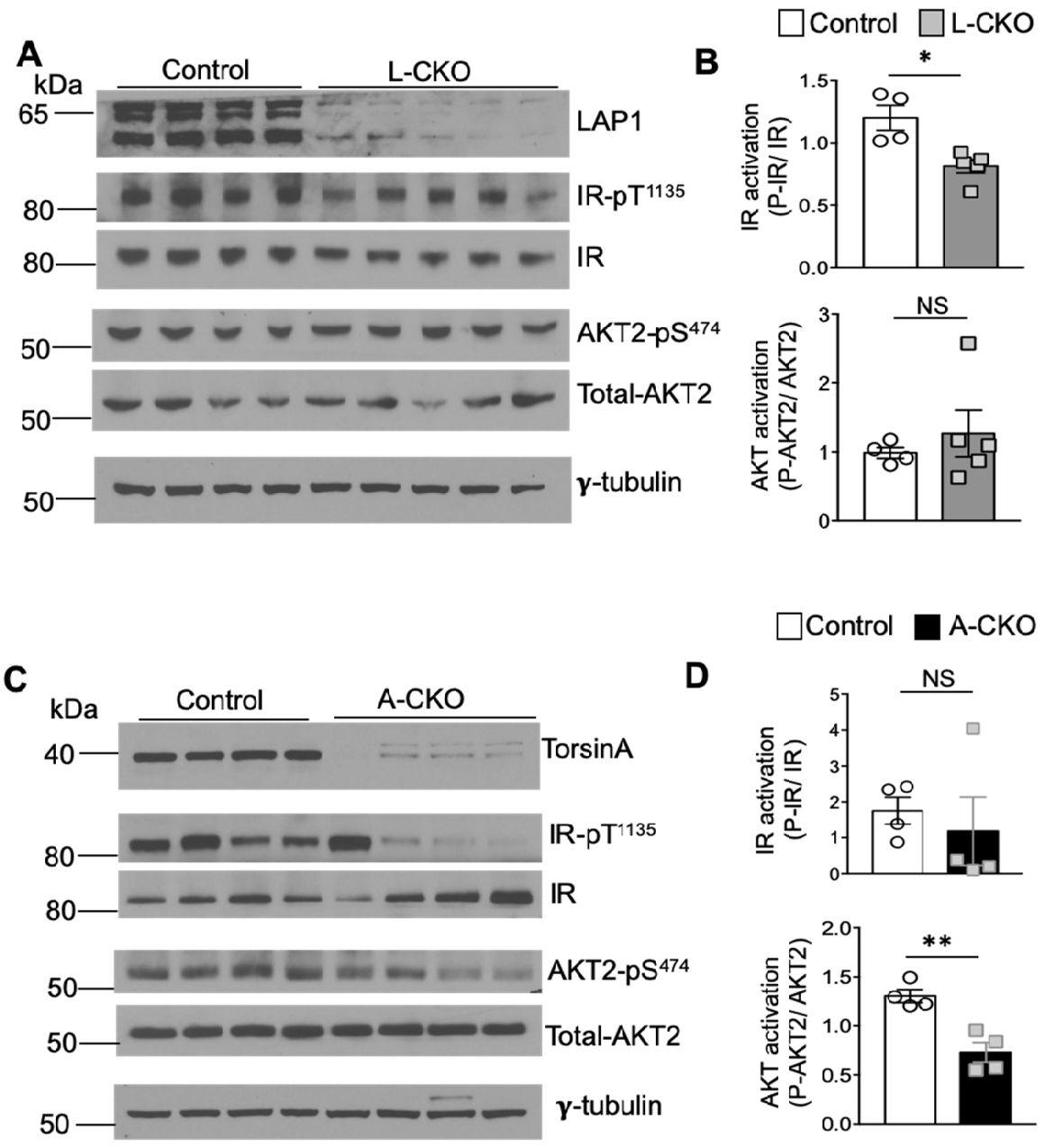

Supplemental Figure 13. Hepatic insulin signaling in L-CKO and A-CKO mice. (A) Immunoblots of liver lysates from control and L-CKO mice using Abs to detect indicated proteins and phosphoproteins; IR: insulin receptor (B) Band densities of indicated proteins were normalized to the band densities of γ-tubulin as a loading control. Activation of IR and AKT2 was calculated from the ratio of phosphoprotein to total protein. Results are from n = 4 control and n

= 5 L-CKO mice. *P < 0.05, NS: not significant by Student's t test. (C) Immunoblots of liver lysates from control and A-CKO mice using Abs to detect indicated proteins involved in IR signaling pathway. (D) Band densities for indicated proteins were normalized to the band densities of γ-tubulin. Activation of IR or AKT2 was calculated from the ratio of phosphorylated proteins/ total proteins. Results are from n = 4 each group. **P < 0.01, NS: not significant by Student's t test. In panels B and D values for individual mice are shown with each bar showing the mean ± SEM. Mice at 4-6 months of age were used.

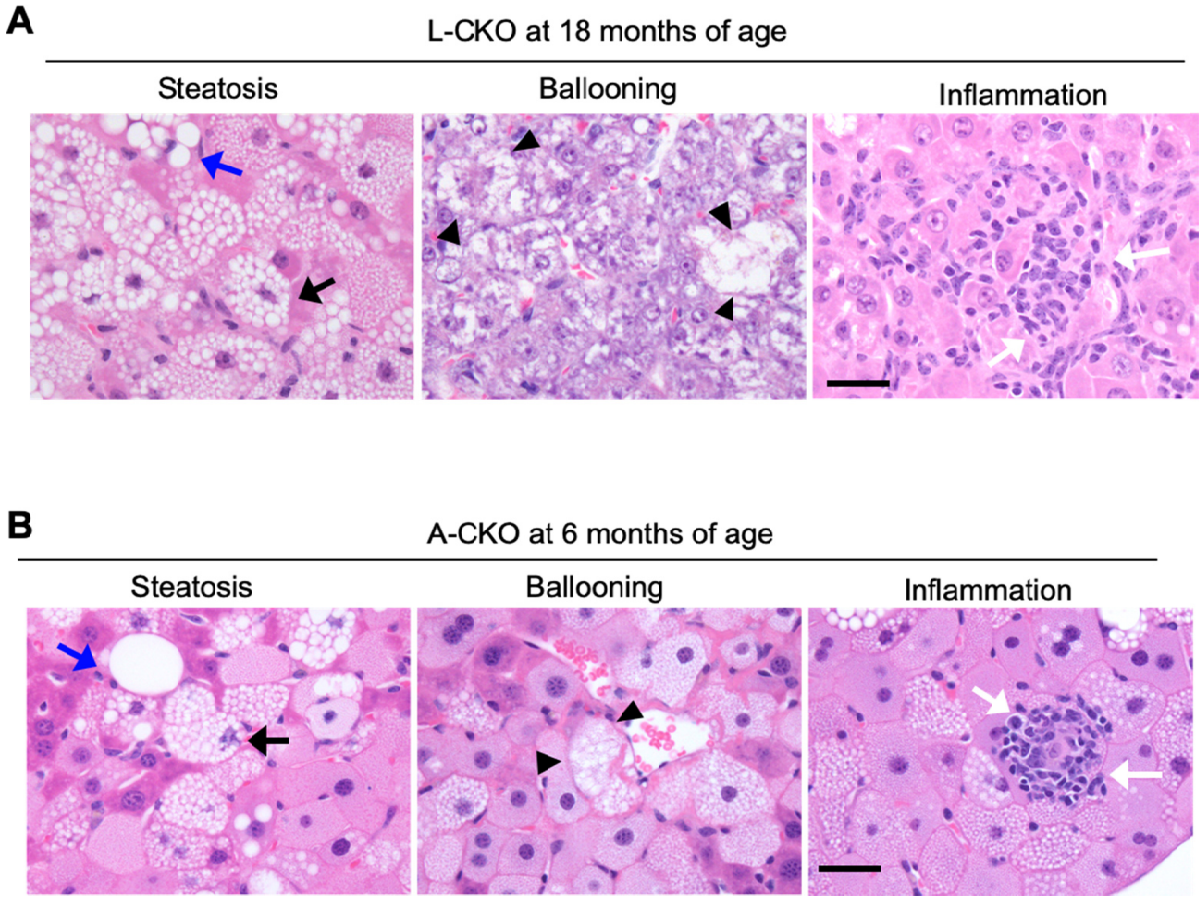

Supplemental Figure 14. Representative photomicrographs of liver sections from L-CKO and A-CKO mice showing features characteristic of NASH. (A) Representative H&E-stained sections of livers from L-CKO mice at 18 months of age. (B) Representative H&E-stained sections of livers from A-CKO mice at 6 months of age. Examples of steatosis, hepatocyte ballooning and inflammation are shown. Macrovesicular steatosis is indicated by blue arrows and microvesicular steatosis indicated by black arrows. Arrow heads indicate hepatocytes with ballooning degeneration. White arrows indicate inflammatory cells. Bars: 50 μm.

Supplemental Table 1. PC/PE ratio from total liver tissues[#]

Control	L-CKO	Control	A-CKO
0.600	0.681	0.812	0.619
0.655	0.441	0.617	0.585
0.693	0.716	0.694	0.586
		0.743	0.596
0.649 ± 0.027	0.613 ± 0.086 ^{NS}	0.716 ± 0.041	0.596 ± 0.008 *

[#]PC and PE levels for each sample are represented as mol % of total lipid composition. The means and standard errors of PC/PE ratios for each genotype are shown in the last row of the table (n=3 for Control and L-CKO, n=4 for Control and A-CKO). *P < 0.05, NS: not significant by unpaired Student's t test.

Supplemental Table 2. Fibrosis stages of liver sections from L-CKO and A-CKO mice[#]

mouse	Control	L-CKO	Control	A-CKO
1	1A	1B	0	1B
2	1A	1A	0	2
3	1A	1B	0	1B
4	1A	1B	1A	2
5		3	0	1A
6		1A	0	2
7		1A		

[#]Firbosis stage for control vs L-CKO mice (2nd and 3rd columns) and control vs A-CKO mice (4th and 5th columns)

Supplemental Table 3. Primer sequences for the lipid metabolism related genes

Gene name	Forward Primer	Reverse Primer
Srebf1	ggc act aag tgc cct caa cct	gcc aca tag atc tct gcc agt gt
Srebf2	cag gga act ctc cca ctt ga	gcc aca tag atc tct gcc agt gt
Acaca	gcc att ggt att ggg gct tac	ccc gac caa gga ctt tgt tg
Fasn	cct gga tag cat tcc gaa cct	agc aca tct gca agg cta cac a
Scd1	tgc gat aca ctc tgg tgc tc	agg ata ttc tcc cgg gat tg
Dgat1	ttc cgc ctc tgg gca tt	aga atc ggc cca caa tcc a
Dgat2	agt ggc aat gct atc atc atc gt	aag gaa taa gtg gga acc cag atc a
apoB	gcc cat tgt gga caa gtg atc	cca gga ctt gga ggt ctt gga
Mttp	aaa gca gag cgg aga cag ag	tat cgc ttt ctg gct gag gt
Ppara	agg gtt gag ctc agt cag ga	ggt cac cta cga gtg gca tt
Ctp1a	cat gtc aag cca aga cga aga	tgg tag gag agc agc acc tt
Aox1	ctt gga tgg tag tcc gga ga	tgg ctt cga gtg agg aag tt